11-1-2011

Measurement Of Magnetic Susceptibility In Pulsed Magnetic Fields Using A Proximity Detector Oscillator

S Ghannadzadeh

M Coak

I Franke

P A. Goddard

J Singleton

See next page for additional authors

Measurement of magnetic susceptibility in pulsed magnetic fields using a proximity detector oscillator

S. Ghannadzadeh,[1,a)] M. Coak,[1] I. Franke,[1] P. A. Goddard,[1] J. Singleton,[2] and J. L. Manson[3]

[1]*Clarendon Laboratory, Department of Physics, University of Oxford, Parks Road, Oxford OX1 3PU, United Kingdom*

[2]*National High Magnetic Field Laboratory, Los Alamos National Laboratory, TA-35, MS-E536, Los Alamos, New Mexico 87545, USA*

[3]*Department of Chemistry and Biochemistry, Eastern Washington University, Cheney, Washington 99004, USA*

(Received 3 September 2011; accepted 29 September 2011; published online 11 November 2011)

We present a novel susceptometer with a particularly small spatial footprint and no moving parts. The susceptometer is suitable for use in systems with limited space where magnetic measurements may not have been previously possible, such as in pressure cells and rotators, as well as in extremely high pulsed fields. The susceptometer is based on the proximity detector oscillator, which has a broad dynamic resonant frequency range and has so far been used predominantly for transport measurements. We show that for insulating samples, the resonance frequency behavior as a function of field consists of a magnetoresistive and an inductive component, originating, respectively, from the sensor coil and the sample. The response of the coil is modeled, and upon subtraction of the magnetoresistive component the dynamic magnetic susceptibility and magnetization can be extracted. We successfully measure the magnetization of the organic molecular magnets $Cu(H_2O)_5(VOF_4)(H_2O)$ and $[Cu(HF_2)(pyz)_2]BF_4$ in pulsed magnetic fields and by comparing the results to that from a traditional extraction susceptometer confirm that the new system can be used to measure and observe magnetic susceptibilities and phase transitions. © *2011 American Institute of Physics*. [doi:10.1063/1.3653395]

I. INTRODUCTION

Radio frequency (RF) techniques have widely been used to measure a range of physical properties.[1–12] Most resonant techniques work by using a simple *LCR* circuit, where either the capacitance or inductance of the tank circuit is coupled to the sample, acting as a probe of its physical properties. Depending on the coupling, changes in the magnetic, dielectric, or conductive properties of the sample can affect the inductance and/or capacitance, which in turn will modify the resonant frequency.

There are several advantages in using RF techniques. The first is that such techniques are contactless, an important consideration for samples where surface contacts can be poor, those which cannot be exposed to the atmosphere for various reasons,[13] or for very small samples where contacts cannot be made easily.[7] Additionally, RF transducers can have extremely high sensitivity due to the high stability of the resonator and the accuracy to which frequency can be measured. Sensitivities down to $1{:}10^9$ have been recorded.[9,14] Also significant is the relatively high speed of data acquisition—signals with frequencies of order of tens of MHz can be digitized directly, and so, changes in sample response can be measured in time scales of 0.1 μs. This is particularly important for experiments in pulsed magnetic fields,[5,15–17] where the pulse duration is typically between 1 ms and 0.5 s.

One of the most widely used of such techniques has been the tunnel diode oscillator (TDO),[18,19] coupled to a sensor coil containing a sample. Despite the high stability of the TDO system under optimum conditions, it has a relatively small stable operating range due to the narrow bias voltage region over which the TDO oscillates.[20–22] A TDO driven circuit is prone to jump to parasitic frequencies and can be taken out of its stable operating condition by changes in the circuit temperature, inductance, and sample size or by the voltages induced in uncompensated coils during experiments using pulsed magnetic fields.[22]

Recently, a new RF circuit, the proximity detector oscillator (PDO), has been reported by Altarawneh, Mielke, and Brooks.[22] The circuit is based on the widely available proximity detector chip that is used in modern metal detectors. It does not suffer from the above issues and can be similarly coupled to a sensor coil containing the sample. The PDO can operate across a wide range of temperatures and inductances, works with coils of various sizes and shapes, has a broad dynamic resonant frequency range, and is insensitive to bias changes.[22] This insensitivity to bias voltages makes the proximity detector system particularly suited for use in pulsed magnetic fields, where significant voltages can be induced due to the high dB/dt. The PDO has successfully been used to measure the skin depths of UIrGe and $Ba_{0.55}K_{0.45}Fe_2As_2$ in high magnetic fields,[23,24] to observe quantum oscillations,[17,25] Fermi-Liquid behavior,[26] and the metal-insulating quantum critical point[16] in $YBa_2Cu_3O_{6+x}$, as well as to investigate the critical field anisotropy[27] of $K_{0.8}Fe_{1.76}Se_2$.

The transport measurements above depend on observing relative changes in the resonator filling factor. The filling factor is defined as the ratio of the volume of the sample penetrated by the RF field, to the overall volume of the RF sensor coil.[28] Thus, in metals the filling factor is

a)Electronic mail: s.ghannadzadeh1@physics.ox.ac.uk.

representative of the skin depth, and in superconductors the penetration depth.[29] Consequently, the PDO, when coupled to an RF sensor coil, is highly sensitive to relative changes in the conductivity of metals and semi-metals—allowing for observation of Shubinkov-de Haas oscillations,[25] as well as superconducting transitions.[24]

While changes in skin/penetration depth dominate the response of metal/superconductors to RF fields, we show in this paper that the magnetic susceptibility[30] dominates the response of insulators. Hence, a PDO system can be used to observe magnetic phase transitions and susceptibility of insulators. We believe that this is the first such application of PDOs.

Therefore, the PDO can be used to observe transport in metals and superconductors, and magnetism in insulators. Being able to probe both properties using a single instrument is highly useful and convenient—there are many systems which have magnetic insulating phases neighboring metallic or superconducting phases in their pressure/temperature phase diagram, such as topological insulators,[31,32] cuprates,[33] and the newly discovered iron chalcogenide[34] superconductors.

We will call our measurement technique/setup, which consists of a sample placed in a sensor coil that is coupled inductively to the proximity detector, a PDO dynamic susceptometer (PDODS), to avoid confusion with the oscillator itself (PDO).

II. ADVANTAGES

There are many advantages to the PDODS. The sensor coil typically consists of only 5–10 turns, and we have used coils with diameters down to 300 μm. Only the sensor coil needs to be placed inside the cryostat—the proximity detector circuit and the power supply can be placed conveniently outside the measurement probe. Thus, the part of PDODS system within the cryostat has a highly compact and small spatial footprint. This, together with the fact that it does not contain any moving parts, means that it is highly suitable for use in systems with limited space where such measurements may not have previously been possible. Such systems include pulsed magnetic fields[24,35] and pressure cells[36,37]—allowing for an exploration of the magnetic, metallic, and superconducting regions of the phase diagram as a function of pressure. For samples where the angle dependent behavior is of interest,[38] the PDODS can also be used in rotators, thus, for example, enabling angle-dependent characterization of anisotropic magnetic systems.

The small spatial footprint means that several sensor coils can be used concurrently on the same measurement probe, even within restrictive pulsed-field magnet bores. This allows for the empty-coil (see Sec. IV) and sample measurements to be performed simultaneously, or even for several samples to be measured during a single pulsed-field experiment. Since typically a cooling time of order an hour[39] is needed between each pulsed-field shot, this can save significant time and expense when compared to a traditional extraction susceptometer, where at least two pulsed shots are needed for each dataset.[40]

Moreover, the lack of moving parts makes the PDODS significantly less sensitive to vibrational noise. This, as well as the insensitivity to dB/dt and the pulse profile (see Sec. VII), makes it suitable for use in multi-stage extremely high pulsed-field (e.g., $H > 70$ T) systems,[39] where a traditional extraction susceptometer has the potential to become unreliable. This insensitivity to vibrational noise, in addition to the possibility of using several sensor coils simultaneously, means that the PDODS may also be suitable for use in multi-mega-gauss destructive single-turn magnets,[41] where the magnet is destroyed after one experiment.

III. EXPERIMENTAL DETAILS

Our measurements were carried out at the Nicholas Kurti High Magnetic Field Laboratory[42] at the University of Oxford. This contains a pulsed-field system capable of reaching fields up to 60 T, with a maximum stored energy of 0.8 MJ. The pulsed field has a variable dB/dt, with rise times to full field ranging from 2.6 ms to 4.6 ms.

The cryostat consists of a large bath of liquid nitrogen used for cooling the magnet, with an insulated space within the magnet bore containing ^{4}He. A simple non-metallic ^{3}He jacket containing the measurement probe is then inserted into the ^{4}He cryostat (see Figure 1). This arrangement allows for temperatures down to 300 mK upon de-pressurisation of the ^{3}He/^{4}He baths.

A schematic diagram of the PDODS circuitry[22] is given in Figure 2. The system uses the commercially available TDA0161 integrated chip (IC) used in metal detectors.[43] The sensor coil is inductively coupled to pins 3 and 7 of the IC, and a proximity detector works by comparing the load impedance R_{3-7} to the resistance R_{2-4} across pins 2 and 4. The IC operating frequency is sustained if $|R_{3-7}| > R_{2-4}$; and when the sensor coil experiences an extra inductive load, the change

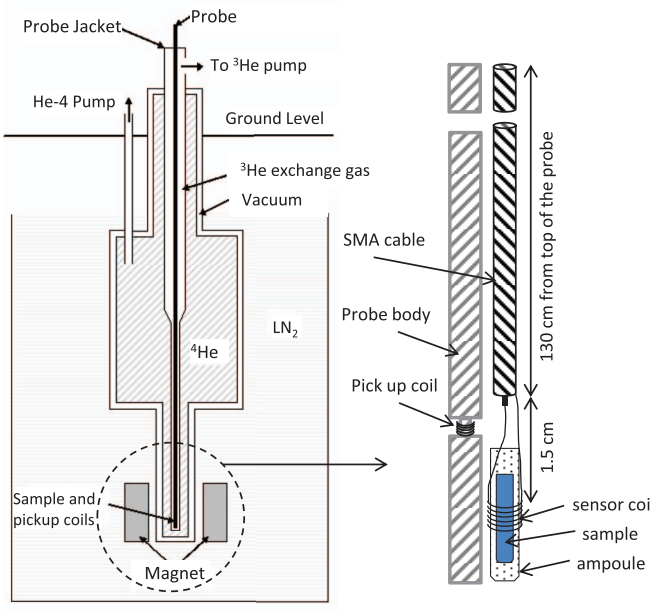

FIG. 1. (Color online) Schematic diagram of the cryostat and PDODS probe design.

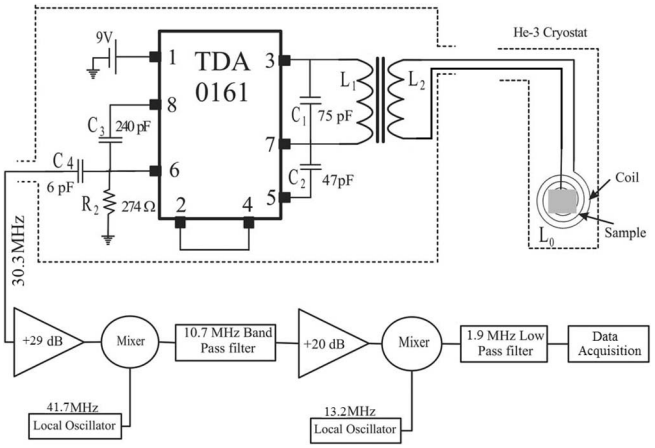

FIG. 2. Schematic diagram of the PDODS system, modified from Altarawneh, Mielke, and Brooks.[22] L_0 is the sensor coil inductance, which is then coupled to the proximity detector chip through inductances L_1 and L_2. C and R represent capacitors and resistors, respectively. $L_2 = L_1 \simeq 0.45\ \mu$H.

in R_{3-7} will modify the current drawn from pin 1.[22,43] This change in current leads to a modification of the metal detector signal.

For our purposes, pins 2 and 4 are short-circuited ($R_{2-4} = 0$) to ensure that the IC will always resonate, and the resonant frequency can be read from the coupling capacitor C_4 on pin 6. Additionally C_3 and R_2 are used to maintain a stable operating voltage, and capacitors C_1 and C_2 are used to tune the resonance frequency to about 30 MHz to allow for measurement of small samples.[22]

Powdered samples are usually held in a 1.3 mm diameter ampoule made of polychlorotrifluoroethylene[44] to allow for easy handling, while single crystal samples are usually used without such protection. To maximise the coupling of the sensor coil to the sample, the sensor coil is made to match the sample or ampoule size and shape as much as possible. The sample/ampoule is placed in the coil, and then mounted on the measurement probe and placed in the cryostat such that the field is parallel to the axis of the coil. Note that the same coil can be used for both transport and magnetic measurements—in metals it is transport that dominates the system response, while in insulators it is magnetism. The PDODS circuitry is then placed at the top of the probe, inside a metallic box for insulation, and is connected to the sensor coil using a semi-rigid sub-miniature version A (SMA) coaxial cable.

The output signal from the proximity detector chip is amplified and undergoes two stage-mixing and filtering to remove high frequency noise. The output is then recorded by a 20 megasamples/s data acquisition card, and the frequency is found by performing a traveling discrete fast Fourier transform with a width of 10 μs. To improve the Fourier transform resolution, extra zeros are added to either side of the time interval (zero padding).[45] Additionally, a simple Hamming window[46] was chosen since only the fundamental frequency is of interest.

Note that the frequency mixing and Fourier transform method explained above is specifically used in pulsed magnetic field due to the very short time interval, to allow for direct digitization of the signal for later analysis. In quasi-static fields, where the time scales are significantly longer, the frequency can be directly recorded by using a frequency counter.

In this paper, the PDODS data are also compared to those taken by a more traditional pulsed field extraction susceptometer. The susceptometer uses a carefully compensated 1500 turn coil, 1.5 mm long and made of high-purity 50 gauge copper wire.[40] During a pulsed magnetic field, the voltage generated in the coil is

$$V \propto -\frac{\mathrm{d}M}{\mathrm{d}t} = -\chi\frac{\mathrm{d}H}{\mathrm{d}t},$$

and so, the dynamic magnetic susceptibility, $\chi = \mathrm{d}M/\mathrm{d}H$, can be found by simply dividing by $\mathrm{d}H/\mathrm{d}t$. The magnetization can then be calculated by numerically integrating this susceptibility.[40] Samples are placed inside ampoules, which can be moved in and out of the susceptometer coil, allowing for more accurate data to be obtained by subtracting the "sample out" background data from the "sample in."

In both the PDODS and the susceptometer probes, the magnetic field is measured by integrating the voltage from an additional 10 turn pick-up coil placed in close proximity to the sample. The pick up coils are calibrated by measuring the de Haas-van Alphen oscillations of the copper coils of the extraction susceptometer.[47]

IV. THEORY

In a system where the sample is inductively coupled to the sensor coil, the inductance L_0 of the coil can be calculated as the sum of the inductances due to the RF field outside and within the skin/penetration depth of the sample,

$$\begin{aligned} L_0 &= L_{\text{space}} + L_{\text{sample}} \\ &= \frac{g}{l}\mu_0\pi N^2(R^2 - r^2) + \frac{g}{l}\mu_0\mu_r\pi N^2[r^2 - (r-\lambda)^2] \\ &= \frac{g}{l}\mu_0\pi N^2[R^2 - r^2 + \mu_r(2r\lambda - \lambda^2)], \end{aligned} \tag{1}$$

where R is the sensor coil radius, r is the sample radius, λ is the sample skin/penetration depth, μ_r is the sample magnetic permeability relative to free space, N is the total number of turns, l is the coil length, and $g \simeq 0.8$ is the geometrical factor[48] for non-infinite coils. We have assumed that both the sample and the coil are cylindrical, that sample length[49] $l_{\text{sample}} \geq l$, and have neglected any edge effects. Differentiating, this gives

$$\Delta L_0 = \frac{g}{l}\mu_0\pi N^2\left[2\mu_r(r-\lambda)\Delta\lambda + (2r-\lambda)\lambda\Delta\mu_r\right].$$

Thus, we can see the effect of changes in the sample skin/penetration depth, which can be used for transport measurements, and changes in relative magnetic permeability, which can be used to probe magnetism.

In metals and superconductors it is changes in the skin/penetration depth $\Delta\lambda$ which dominate the coil inductance. However, in insulators the RF field penetrates the whole of the sample—in effect loading the coil with a constant volume,[20] and so the system becomes insensitive to changes

in the skin/penetration depth. In this case, small changes in the magnetic permeability μ_r can become significant.

Therefore, setting $\Delta\lambda = 0$ and $\lambda = r$ for insulators,[50] Eq. (1) can be reduced to

$$L_0 = \frac{g}{l}\mu_0\pi N^2(R^2 - r^2 + \mu_r r^2) = L_{\text{empty}}(1 + f\chi)$$

and

$$\Delta L_0 = L_{\text{empty}} f \Delta\chi, \tag{2}$$

where $L_{\text{empty}} = g\mu_0\pi R^2 N^2/l$ is the empty coil inductance, $f = r^2/R^2$ is the coil filling factor, and $\chi = \mu_r - 1 = \mathrm{d}M/\mathrm{d}H$.

Applying circuit theory to the schematic in Figure 2, one has

$$V = I_1 R_1 + L_1\frac{\mathrm{d}I_1}{\mathrm{d}t} - m\frac{\mathrm{d}I_0}{\mathrm{d}t}, \tag{3}$$

$$0 = R_0 I_0 + L_0\frac{\mathrm{d}I_0}{\mathrm{d}t} - m\frac{\mathrm{d}I_1}{\mathrm{d}t} + L_2\frac{\mathrm{d}I_0}{\mathrm{d}t}, \tag{4}$$

where R_0 is the sensor coil and coax cable resistance, R_1 is the resistance of inductor L_1, m is coupling factor between L_1 and L_2, I_0 and I_1 are the currents through inductors L_0 and L_1, and V is the voltage across pins 3 and 7 of the proximity detector chip.

Substituting Eq. (4) into (3), and setting $I_0 \propto I_1 \propto \exp(j\omega t)$, we have

$$V = \left[R_1 + j\omega L_1 + \frac{m^2\omega^2}{R_0 + j\omega(L_0 + L_2)}\right] I_1. \tag{5}$$

By considering the imaginary component of the above equation, one gets the effective inductance of the circuit,

$$L_{\text{eff}} = L_1\left[1 - \frac{m^2\omega^2}{R_0^2 + \omega^2(L_2 + L_0)^2}\left(\frac{L_0 + L_2}{L_1}\right)\right]. \tag{6}$$

Being an *LCR* circuit, the overall angular resonance frequency is then[29]

$$\omega = \frac{1}{\sqrt{L_{\text{eff}}C}},$$

in which C is the overall circuit capacitance. We can differentiate to obtain

$$\frac{\Delta\omega}{\omega} = -\frac{\Delta L_{\text{eff}}}{2L_{\text{eff}}}, \tag{7}$$

where $\Delta\omega = \omega(H) - \omega$ is the change in resonant frequency when a magnetic field H is applied, and similarly $\Delta L_{\text{eff}} = L(H) - L_{\text{eff}}$.

Substitution of Eq. (6) into the above equation results in a rather complicated expression, which upon assuming small changes in variables[51] ($\Delta\omega \ll \omega$, $\Delta L_0 \ll L_0$, $\Delta R_0 \ll R_0$) results in

$$\Delta\omega = -a\Delta L_0 - b\Delta R_0, \tag{8}$$

where a, b are positive constant functions of R_0, ω, C, and the inductances, and ΔR_0 represents the magnetoresistance of the coax cable and the sensor coil in the presence of a magnetic field.

Finally, after substituting Eq. (2), one can relate changes in the dynamic susceptibility of insulating samples to frequency

$$\Delta\omega = -a'\Delta\chi - b\Delta R_0, \tag{9}$$

where $a' = af L_{\text{empty}}$.

We can isolate the susceptibility by taking a background measurement, where an identical empty coil is used. In that case, assuming that changes in the permeability of the exchange medium are negligible, we can set $\Delta\chi = 0$, to get

$$\Delta\omega_{\text{background}} = -b\Delta R_0. \tag{10}$$

By subtracting the background measurement from that with the sample,

$$\Delta\chi = \frac{1}{a'}(\Delta\omega_{\text{background}} - \Delta\omega_{\text{with sample}}) \tag{11}$$

and setting $\Delta\chi = \chi(H) - \chi_0$, where χ_0 is a constant, we get

$$\chi(H) = \frac{1}{a'}(\Delta\omega_{\text{background}} - \Delta\omega_{\text{with sample}}) + \chi_0. \tag{12}$$

V. MAGNETORESISTANCE OF CIRCUIT ELEMENTS

The response of the PDO, when coupled to empty coils made from aluminum or copper, is shown in Figure 3 as a function of field. The changes in ω can be attributed to magnetoresistance and other second-order effects not considered in the previous calculations.[52]

The magnetoresistance background of a coil can be approximated as

$$\Delta\omega_{\text{background}} = -b\Delta R_0 = \frac{\alpha}{H^{-2} + \beta} + \gamma H^2 + \eta H, \tag{13}$$

where α, β, γ, and η are constants. The first and second terms, respectively, represent the closed and open quasi-particle orbits around the Fermi surface[53] in the limit $\omega_c\tau \to \infty$ (ω_c

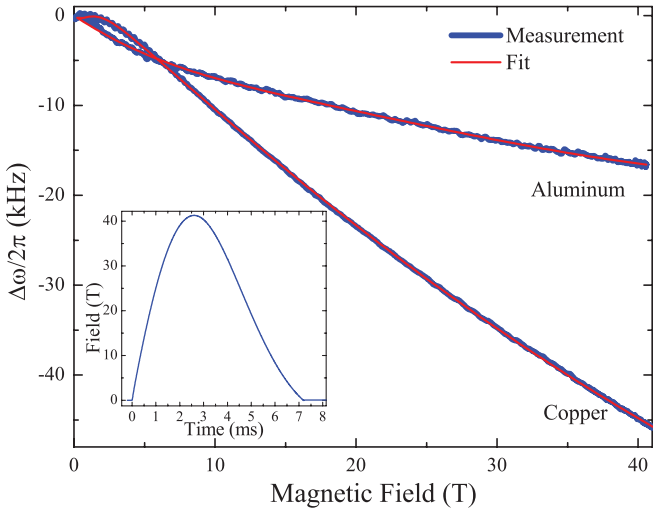

FIG. 3. (Color online) Relative shift in resonant frequency at 4.2 K when using coils made with: 8 turns of 75 μm copper or 100 μm aluminum wire. Also plotted are least-squares fits using Eq. (13). Inset: time profile of a typical field pulse.

TABLE I. Parameters from least-square fits of Eq. (13) to the frequency response of empty copper and aluminum coils.

	Copper	Aluminum
$\alpha/2\pi$ (Hz/T^2)	2050	31.43
β (T^{-2})	0.5	0.0022
$\gamma/2\pi$ (Hz/T^2)	7.45	8.83
$\eta/2\pi$ (Hz/T)	−1520	−1041

is the cyclotron frequency, τ is the relaxation time). The last term is a phenomenological term associated with linear transverse magnetoresistance at high magnetic fields.[54–56] As shown in Figure 3, this equation closely matches the background response of both copper and aluminum coils. The list of fit parameters is given in Table I. The magnetoresistance was found to be largely temperature independent below 20 K.

From Figure 3, it is clear that aluminum has a considerably lower magnetoresistance than copper. However, it still may be desirable to use copper in some applications (such as pressure cells) due to its superior structural and tensile properties, and the ease with which electrical contacts are applied.

VI. SAMPLES

The first sample to be measured by the PDODS is a single crystal of $Cu(H_2O)_5(VOF_4)(H_2O)$.[57] This material has a magnetic behavior similar to a spin-gap or a dimer system.[58] At low temperatures ($T < 4$ K), the magnetization is close to zero up to around 13 T, at which point it undergoes a very sharp and well-defined magnetic transition, leading to a saturation magnetization of $2.3\mu_B$/formula-unit. The height of this transition is reduced with increasing temperature, and it eventually disappears at $T \approx 10$K to give way to a gradual rise in magnetization. This material is, therefore, ideal for testing the response of the PDODS to sharp magnetic transitions, as well as more gradual variations in magnetization, as a function of the magnetic field.

The second material to be measured is a powdered sample of the metal-organic coordination polymer $[Cu(HF_2)(pyz)_2]BF_4$. This is a well-studied[40] quasi-two-dimensional Heisenberg antiferromagnet, with gyromagnetic g-factor of 2.13, exchange coupling $|J|$ of 6.3 K, exchange anisotropy $|J_\perp/J|$ of 9×10^{-4}, and a Néel temperature of 1.54 K. This system shows a gradual concave rise in magnetization with increasing field, saturating at 18 T.

VII. SUSCEPTIBILITY

A $1.5 \times 0.6 \times 0.3$ mm^3 single crystal of $Cu(H_2O)_5(VOF_4)(H_2O)$ was placed in an ampoule and measured using an 8 turn coil made of 100 μm aluminum thick wire, with coil diameter of 1.3 mm. Measurements were done at a range of temperatures, a selection of which are shown in Figure 4(a).

Equation (9) implies that $\Delta\omega \propto -\Delta\chi$, and the changes in magnetic susceptibility are quite clear at low temperatures without any need to subtract the background or perform any further analysis: relative frequency shifts of about 4 kHz are seen at 12 T and 20 T, representing the magnetic transition. Also note how this transition is no longer seen at 20 K implying that at high temperatures the changes in the magnetization are much more gradual.

The data with the background subtracted are shown in Figure 4(b). The magnetic transition at low temperatures is well pronounced, and the resonant frequency is shown to be constant at $H < 13$ T and $H > 20$ T—in these regions we know there is no change in the magnetization, implying $\chi = 0$. However, $\Delta\omega$ is still non-zero due to the χ_0 constant term in Eq. (12).

The data from a traditional extraction susceptometer are shown in Figure 4(c), for the same sample. It is clear that both PDODS and the susceptometer data are qualitatively very similar.

The PDODS response to powdered sample of $[Cu(HF_2)(pyz)_2]BF_4$ was similarly measured using a coil of 6 turns of 100 μm aluminum wire, and is shown in

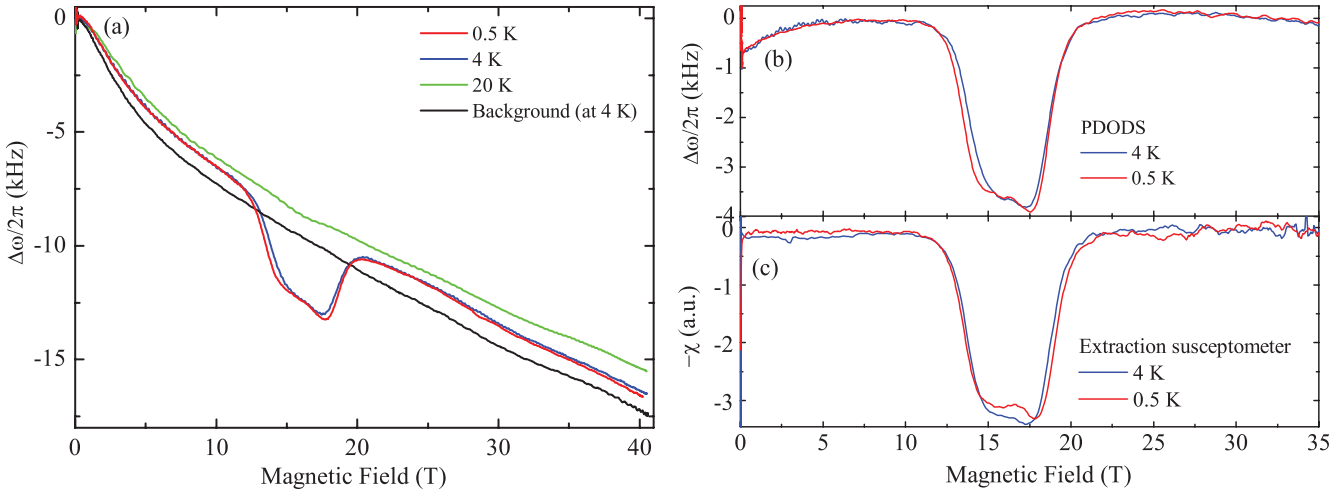

FIG. 4. (Color online) (a) PDODS frequency shifts for the sample $Cu(H_2O)_5(VOF_4)(H_2O)$ at various temperatures. Some smoothing has been performed to reduce high frequency noise. (b) PDODS frequency shift with the background and the $a'\chi_0$ constant removed. (c) Data from the extraction susceptometer.

inset of Figure 6. As expected, $\Delta\omega$ varies smoothly at low fields, and a sudden change is seen at around 18 T as the system becomes saturated. This sample was also measured using the traditional extraction susceptometer, and it also showed the same behavior.

In addition, both samples were measured with magnetic pulses of different magnitudes with rise times ranging from 2.6 μs to 4.6 μs, corresponding to dB/dT varying from 4.7 T/ms to 16 T/ms, and no change was observed in the PDODS behavior at such rates. $Cu(H_2O)_5(VOF_4)(H_2O)$ was also measured successfully in an Oxford Instruments 17 T superconducting magnet, and similar features were seen.

In summary, the fact that the PDODS and the extraction susceptometer data look the same for both samples shows that χ dominates the resonator response, and so, the PDODS system can be used for dynamic susceptibility measurements in insulators.

VIII. MAGNETIZATION

Once the background is removed from the data, the magnetization can be calculated from Eq. (12) by subtracting a constant corresponding to the $a'\chi_0$ term and then numerically integrating. In samples which saturate during the pulse, the susceptibility should be zero after saturation, and so, any nonzero susceptibility can be attributed to this $a'\chi_0$. For samples which do not saturate fully, the correct $a'\chi_0$ can be found by comparing the PDODS results to low field data from other magnetometers, such as a SQUID magnetometer (for which commercial pressure cells are available).[59]

Both of the samples measured above become saturated at high fields, and at 4 K $a'\chi_0/2\pi$ is found to be around 0.75 kHz for $Cu(H_2O)_5(VOF_4)(H_2O)$ and 0.5 kHz for $[Cu(HF_2)(pyz)_2]BF_4$.

A comparison is made between the PDODS and extraction susceptometer magnetization data for $Cu(H_2O)_5(VOF_4)(H_2O)$ in Figure 5. The PDODS data agree very well with the susceptometer, successfully showing the sharp magnetic transition at low temperatures, as well as the more gradual change in magnetization at higher temperatures. Further measurements were taken at several temperatures in between 0.5 K and 20 K, and they show similar agreement.

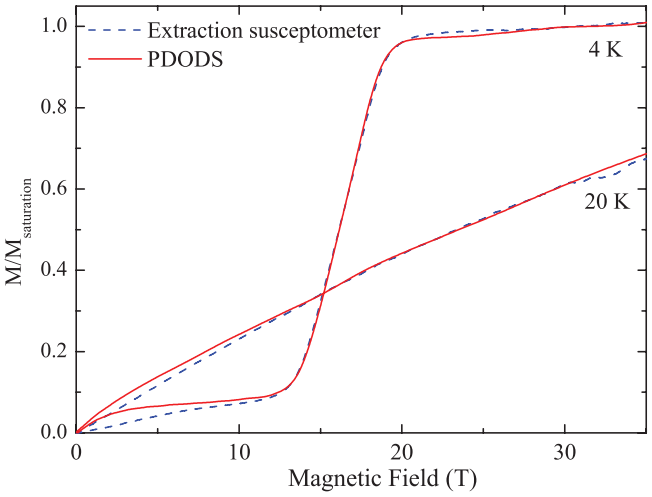

FIG. 5. (Color online) Comparison of the deduced magnetization from the PDODS and the extraction susceptometer data, for $Cu(H_2O)_5(VOF_4)(H_2O)$ at 4 K and 20 K.

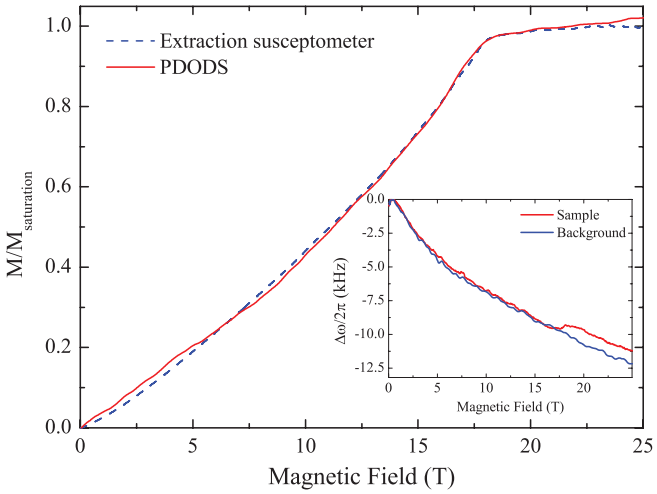

FIG. 6. (Color online) Magnetization of the metal-organic coordination polymer[40] $[Cu(HF_2)(pyz)_2]BF_4$ at 1.5 K, using the PDODS and the extraction susceptometer. Inset: relative change in the PDODS resonant frequency during the pulse.

Similarly, the integrated magnetization for $[Cu(HF_2)(pyz)_2]BF_4$ is given in Figure 6. Once again, the extraction susceptometer and the PDODS agree very well—we see a gradual concave rise in magnetization typical of quasi-two-dimensional magnets, leading to a sharp transition at 18 T which has been rounded slightly because of the powdered average of the anisotropic g-factor.[40]

The absolute magnetization can be found by comparing the PDODS results with respect to low temperature data from other magnetometers, such as a SQUID. Alternatively, for samples which saturate, one can normalize the magnetization by the saturation value. Calibrating the PDODS in such ways is not a disadvantage, as all magnetometers, such as AC susceptometers, vibrating sample magnetometers, and even modern SQUIDs, need to be similarly calibrated by using reference magnetic samples.

IX. CONCLUSION

In this paper, we have successfully explained the resonant frequency behavior of the proximity detector oscillator as a function of magnetic field when coupled inductively to a sensor coil containing an insulating sample. The frequency response consists of a magnetoresistive component, which was modeled for copper and aluminum coils, and an inductive component, which can be related to the coil filling factor and the dynamic magnetic susceptibility of the sample.

It was shown that for the two insulating samples $Cu(H_2O)_5(VOF_4)(H_2O)$ and $[Cu(HF_2)(pyz)_2]BF_4$, the magnetic susceptibility dominates the inductance of the measurement coil, and that upon careful subtraction of the magnetoresistance background, the magnetic susceptibility

and magnetization can be measured—in agreement with data from a traditional extraction susceptometer.

In summary, we have shown that the proximity detector oscillator dynamic susceptomter is highly suitable for measurement of magnetization and magnetic transitions in insulators. This, together with the small spatial footprint of the measurement coil, makes it highly adaptable for use in pressure cells for examination of materials with metallic-insulating phase transitions—allowing transport and magnetization to be measured in the conducting and insulating phases, respectively, and giving way for a full characterization of the phase diagram as function of pressure, magnetic field, and temperature.

ACKNOWLEDGMENTS

The authors would like to thank M. M. Altarawneh and C. H. Mielke for helpful discussions. This work is supported by the EPSRC (UK).

[1] J. D. Fletcher, A. Carrington, P. Diener, P. Rodière, J. P. Brison, R. Prozorov, T. Olheiser, and R. W. Giannetta, Phys. Rev. Lett. **98**, 057003 (2007).
[2] J. D. Fletcher, A. Carrington, O. J. Taylor, S. M. Kazakov, and J. Karpinski, Phys. Rev. Lett. **95**, 097005 (2005).
[3] F. Manzano, A. Carrington, N. E. Hussey, S. Lee, A. Yamamoto, and S. Tajima, Phys. Rev. Lett. **88**, 047002 (2002).
[4] S. E. Sebastian, J. Gillett, N. Harrison, P. H. C. Lau, D. J. Singh, C. H. Mielke, and G. G. Lonzarich, J. Phys.: Condens. Matter **20**, 422203 (2008).
[5] E. A. Yelland, J. Singleton, C. H. Mielke, N. Harrison, F. F. Balakirev, B. Dabrowski, and J. R. Cooper, Phys. Rev. Lett. **100**, 047003 (2008).
[6] T. A. Olheiser, Z. Shi, D. D. Lawrie, R. W. Giannetta, and J. A. Schlueter, Phys. Rev. B **80**, 054519 (2009).
[7] R. Prozorov, M. D. Vannette, G. D. Samolyuk, S. A. Law, S. L. Bud'ko, and P. C. Canfield, Phys. Rev. B **75**, 014413 (2007).
[8] S. E. Sebastian, N. Harrison, C. H. Mielke, R. Liang, D. A. Bonn, W. N. Hardy, and G. G. Lonzarich, Phys. Rev. Lett. **103**, 256405 (2009).
[9] E. Ohmichi, E. Komatsu, and T. Osada, Rev. Sci. Instrum. **75**, 2094 (2004).
[10] W. A. Coniglio, L. E. Winter, K. Cho, C. C. Agosta, B. Fravel, and L. K. Montgomery, Phys. Rev. B **83**, 224507 (2011).
[11] J. Singleton, Rep. Prog. Phys. **63**, 1111 (2000).
[12] M.-S. Nam, J. Singleton, A.-K. Klehe, W. Hayes, M. Kurmoo, and P. Day, in *Proceedings of the International Conference on Science and Technology of Synthetic Metals*, 1998, Montpellier, France [Synth. Met. **103**, 2259 (1999)].
[13] K. Cho, H. Kim, M. A. Tanatar, Y. J. Song, Y. S. Kwon, W. A. Coniglio, C. C. Agosta, A. Gurevich, and R. Prozorov, Phys. Rev. B **83**, 060502 (2011).
[14] A. Carrington, R. W. Giannetta, J. T. Kim, and J. Giapintzakis, Phys. Rev. B **59**, R14173 (1999).
[15] C. Mielke, J. Singleton, M.-S. Nam, N. Harrison, C. C. Agosta, B. Fravel, and L. K. Montgomery, J. Phys.: Condens. Matter **13**, 8325 (2001).
[16] S. Sebastian, N. Harrison, M. Altarawneh, C. Mielke, R. Liang, D. Bonn, and G. Lonzarich, Proc. Natl. Acad. Sci. U.S.A. **107**, 6175 (2010).
[17] J. Singleton, C. de la Cruz, R. D. McDonald, S. Li, M. Altarawneh, P. Goddard, I. Franke, D. Rickel, C. H. Mielke, X. Yao, and P. Dai, Phys. Rev. Lett. **104**, 086403 (2010).
[18] C. Boghosian, H. Meyer, and J. E. Rives, Phys. Rev. **146**, 110 (1966).
[19] G. J. Athas, J. S. Brooks, S. J. Klepper, S. Uji, and M. Tokumoto, Rev. Sci. Instrum. **64**, 3248 (1993).
[20] T. Coffey, Z. Bayindir, J. F. DeCarolis, M. Bennett, G. Esper, and C. C. Agosta, Rev. Sci. Instrum. **71**, 4600 (2000).
[21] C. T. V. Degrift and D. P. Love, Rev. Sci. Instrum. **52**, 712 (1981).
[22] M. M. Altarawneh, C. H. Mielke, and J. S. Brooks, Rev. Sci. Instrum. **80**, 066104 (2009).
[23] F. Nasreen, K. Kothapalli, M. M. Altarawneh, H. Nakotte, N. Harrison, and E. Brück, J. Phys.: Conf. Ser. **273**, 012154 (2011).
[24] M. M. Altarawneh, K. Collar, C. H. Mielke, N. Ni, S. L. Bud'ko, and P. C. Canfield, Phys. Rev. B **78**, 220505 (2008).
[25] S. E. Sebastian, N. Harrison, P. A. Goddard, M. M. Altarawneh, C. H. Mielke, R. Liang, D. A. Bonn, W. N. Hardy, O. K. Andersen, and G. G. Lonzarich, Phys. Rev. B **81**, 214524 (2010).
[26] S. E. Sebastian, N. Harrison, M. M. Altarawneh, R. Liang, D. A. Bonn, W. N. Hardy, and G. G. Lonzarich, Phys. Rev. B **81**, 140505 (2010).
[27] E. D. Mun, M. M. Altarawneh, C. H. Mielke, V. S. Zapf, R. Hu, S. L. Bud'ko, and P. C. Canfield, Phys. Rev. B **83**, 100514 (2011).
[28] T. Coffey, "Novel metals, magnets, and measurements: The critical magnetic field phase diagram of an organic conductor," Ph.D. dissertation, Clark University, 2003.
[29] B. Bleaney and B. Bleaney, *Electricity and Magnetism* (Oxford University Press, New York, 1976).
[30] In early application of TDO-driven RF coils to organic metals and superconductors, it was assumed that changes in susceptibility would dominate the response, and that the quantum oscillations observed were de Haas-van Alphen oscillations (Refs. 11, 12, and 19). Subsequent experience has showed that it is the skin depth changes that dominate, and that the quantum oscillations observed were Shubnikov-de Haas instead (Refs. 9, 15, and 20).
[31] D. Hsieh, D. Qian, L. Wray, Y. Xia, Y. S. Hor, R. J. Cava, and M. Z. Hasan, Nature (London) **452**, 970 (2008).
[32] M. Z. Hasan and C. L. Kane, Rev. Mod. Phys. **82**, 3045 (2010).
[33] J. Orenstein and A. J. Millis, Science **288**, 468 (2000).
[34] M.-H. Fang, H.-D. Wang, C.-H. Dong, Z.-J. Li, C.-M. Feng, J. Chen, and H. Q. Yuan, Europhys. Lett. **94**, 27009 (2011).
[35] J. Singleton, C. Mielke, A. Migliori, G. Boebinger, and A. Lacerda, in *Proceedings of the 7th International Symposium on Research in High Magnetic Fields*, Toulouse, France, 2003 [Physica B **346–347**, 614 (2004)].
[36] N. Suresh and J. L. Tallon, J. Phys.: Conf. Ser. **121**, 052004 (2008).
[37] K. M. Purcell, D. Graf, M. Kano, J. Bourg, E. C. Palm, T. Murphy, R. McDonald, C. H. Mielke, M. M. Altarawneh, C. Petrovic, R. Hu, T. Ebihara, J. Cooley, P. Schlottmann, and S. W. Tozer, Phys. Rev. B **79**, 214428 (2009).
[38] P. A. Goddard, J. Singleton, A. L. Lima Sharma, E. Morosan, S. J. Blundell, S. L. Bud'ko, and P. C. Canfield, Phys. Rev. B **75**, 094426 (2007).
[39] J. Sims, A. Baca, G. Boebinger, H. Boenig, H. Coe, K. Kihara, M. Manzo, C. Mielke, J. Schillig, Y. Eyssa, B. Lesch, L. Li, and H. Scneider-Muntau, IEEE Trans. Appl. Supercond. **10**, 510 (2000).
[40] P. A. Goddard, J. Singleton, P. Sengupta, R. D. McDonald, T. Lancaster, S. J. Blundell, F. L. Pratt, S. Cox, N. Harrison, J. L. Manson, H. I. Southerland, and J. A. Schlueter, New J. Phys. **10**, 083025 (2008).
[41] C. Mielke and R. McDonald, in *Proceedings of the IEEE International Conference on Megagauss Magnetic Field Generation and Related Topics, Santa Fe, NM, 5–10 November 2006* (IEEE, Piscataway, NJ, 2006), p. 227.
[42] H. Witte and H. Jones, in *Proceedings of the 7th International Symposium on Research in High Magnetic Fields*, Toulouse, France, 2003 [Physica B **346–347**, 663 (2004)].
[43] ST Microelectronics, "TDA0161 proximity detector," www.st.com.
[44] A. Mari and L. Brossard, Rev. Sci. Instrum. **64**, 1364 (1993).
[45] L. Drigo, F. Durantel, A. Audouard, and G. Ballon, Eur. Phys. J.: Appl. Phys. **52**, 10401 (2010).
[46] F. Harris, Proc. IEEE **66**, 51 (1978).
[47] J. A. Detwiler, G. M. Schmiedeshoff, N. Harrison, A. H. Lacerda, J. C. Cooley, and J. L. Smith, Phys. Rev. B **61**, 402 (2000).
[48] W. Duffin, *Electricity and Magnetism* (McGraw-Hill College, Maidenhead, England, 1990).
[49] If $l_{\text{sample}} \leq l$ instead, then Eq. (1) is scaled by l_{sample}/l and a constant $g\mu_0\pi N^2 R^2(l - l_{\text{sample}})/l^2$ is also added to inductance. Equation (2) then becomes $\Delta L_0 = l_{\text{sample}} L_{\text{empty}} f \Delta\chi/l$. Thus, all equations still hold, but with a scaling of l_{sample}/l.
[50] In reality $\lambda \gg r$; however, for the purposes of Eq. (1), we have to set $\lambda = r$.
[51] This assumption is valid as typical changes in $\omega/2\pi$ is of order of 10 s of KHz, while $\omega/2\pi$ itself is about 30 MHz.
[52] This background can also include a noticeable drop in frequency at low fields due to the superconducting transition of the solder used. Here, a 60%/40% Tin/Lead solder was used which has a critical field $H_c = 0.08$ T and transition temperature $T_c = 7.05$ K.
[53] J. Singleton, *Band Theory and Electronic Properties of Solids* (Oxford University Press, New York, 2001).
[54] J. de Launay, R. Dolecek, and R. Webber, J. Phys. Chem. Solids **11**, 37 (1959).

[55]P. Kapitza, Proc. R. Soc. London, Ser. A **123**, 292 (1929).
[56]F. Fickett, in *Proceedings of the Fourth International Conference on Magnet Technology, Upton, NY, 1972* (Brookhaven National Laboratory, Upton, NY, 1972), p. 539.
[57]J. L. Manson, *et al*. (to be published).
[58]H. Kageyama, K. Yoshimura, R. Stern, N. V. Mushnikov, K. Onizuka, M. Kato, K. Kosuge, C. P. Slichter, T. Goto, and Y. Ueda, Phys. Rev. Lett. **82**, 3168 (1999).
[59]Qunatum Design USA, High pressure cell kit for the MPMS, www.qdusa.com.